 doi:10.20944/preprints201811.0385.v1

Article

Development of a stoichiometric model for estimation of metabolic fluxes in *Saccharomyces cerevisiae* during tequila production

José Daniel Padilla-de la R. [1], Anne Gschaedler-M.[1] , Abril Gomez-G[2] and Orfil González-R.[2,*]

[1] Centro de Investigación y Asistencia Tecnológica y Diseño del Estado de Jalisco (CIATEJ), Av. Normalistas No. 800, C.P. 44720, Guadalajara, Jalisco, México; www.ciatej.net.mx
[2] Departamento de Ingeniería Química, CUCEI, Universidad de Guadalajara. Blvd. Marcelino García Barragán #1421, esq. Calzada Olímpica, C.P. 44430 Guadalajara, Jalisco, México; www.udg.mx
* Correspondence: orfil.gonzalez@cucei.udg.mx; Tel.: +01-331-378-5900 Ext# 27508

Abstract: In this study is developed an aerobic and anaerobic stoichiometric model for *Saccharomyces cerevisiae*, compartmentalized in mitochondria and cytosol. This model considers the central metabolism of *S. cerevisiae* and it possesses the peculiarity of having catabolic and anabolic biochemical reactions for the synthesis of the higher alcohols contained in tequila; involving 94 metabolites and 117 reactions; of which 93 correspond to biochemical internal reactions and 24 to transport fluxes between the medium and the cell. The model is validated under aerobic and anaerobic conditions for the main fermentation metabolites and it coincides with experimental results and those *in silico* reported in the literature. This model is used to obtain three different physiological states of *S. cerevisiae* through of estimation of its distributions of fluxes calculated from experimental data reported in literature of fermentation in continuous culture during the tequila production under different dilution rate (0.04-0.12 h^{-1}). The model developed constitutes a tool for the estimation of flux distribution maps during fermentation processes for the production of tequila, which could permit estimate yields and visualize different fermentation scenarios.

Keywords: Flux Balance Analysis, *Saccharomyces cerevisiae*, Tequila, fermentation, higher alcohols.

1. Introduction

Tequila is a regional alcoholic beverage typically Mexican recognized at the worldwide level. This beverage is obtained from *Agave tequilana* Weber blue variety, which is cultivated in the denomination-of-origin zone, according to the Official Mexican Norm Regulation (NOM-006-SCFI-2012)[1]. The production process consists of five stages: cooking, grinding, fermentation, distillation and, resting or aging [2]. From these stages, the fermentation is one of the most important in the process of tequila production; during this process the sugars (principally fructose) are metabolized into ethanol, Carbon dioxide (CO_2), and also into a great variety of secondary products, such as the volatile compounds involved in the tequila bouquet [3].

The Official Mexican Norm Regulation (NOM-006-SCFI-2012)[1], also regulates the maximal permissible concentration of higher alcohols which must be 500 mg/100 ml of anhydrous alcohol; however, compliance with the norm is one of the main problems that exists in the tequila industry.

 doi:10.20944/preprints201811.0385.v1

The aroma of the tequila depends on the amount and type of volatile compounds present in it. Even that more than 200 volatile compounds have been identified; only a few of them play a decisive role in the tequila bouquet [4]. This composition can be affected by different factors, such as the composition of the fermentation medium and the metabolism of the yeast. In the specific case of the production of higher alcohols, the composition of the tequila can be affected by the amount and type of the nitrogen source and the way in which it is metabolized by the yeast [3,5,6].

Saccharomyces cerevisiae is the microorganism commonly employed to ferment the agave-juice in a batch process. Also, *S. cerevisiae* is one of the most studied microorganisms; there is considerable amount of information about its metabolism [7]; it has been demonstrated to be very versatile microorganism in terms of industrial applications; therefore, it is interesting for metabolic engineering studies [7]. From its sequencing, various classes of analysis have been applied with the purpose of elucidating the function of its genes, integration and, metabolism [8]. One way to study its physiology is using the Genomic Scale Models (GSM) to estimate its metabolic fluxes. GSM comprise mathematical representations of a metabolic networks and they have been used to model underlying processes and biological phenotypes of many organisms [9]. GSM are collections of biochemical reactions stoichiometrically annotated related with their enzymes in a cell/tissue [10]. The applications of GSM are multiple, but commonly they include analysis of topological networks and the integration of omics data, or the prediction of phenotypes by means of metabolism simulations, with the objective of designing metabolic engineering strategies [11]. These models allow the proposal and testing of novel hypotheses on metabolic functions in the organism-of-interest. Thus, there has been growing interest in the reconstruction of metabolic networks and in the scope of their applications [12]. More than 100 GSM networks have been built for a very broad range of different microorganisms of the different kingdoms: bacteria, eukaryotes and archea [13]. For example, *Haemophilus influenzae*, *Escherichia coli*, *Saccharomyces cerevisiae*, *Helicobacter pylori*, *Staphyloccocus aureus*, *Bacillus subtilis*, *Homo sapiens*, *Pseudomona aeruginosa*, and for the genus *Synechocystis*, among others [12].

Particularly, for *Saccharomyces cerevisiae*, various GSM have been reported in the literature over the past decade [7], including the following: iFF708 [14]; iND750 [15]; iLL672 [16]; iIN800 [17], iMM904 [18]; iTO977 [19], and Yeast 6 [20]. Over the years, each of these models have incorporated an increasing number of Open Reading Frames (ORF), reactions, and compartments. Thus, the first version, iFF708, contains 708 ORF, with 1,175 reactions and three compartments, while the most recent version, Yeast 6, contains 900 ORF, with 1,888 reactions and 15 compartments [7]. In this study is developed an aerobic and anaerobic stoichiometric model for *Saccharomyces cerevisiae*, compartmentalized in mitochondria and cytosol. This model considers the central metabolism of *S. cerevisiae* and it possesses the peculiarity of having catabolic and anabolic biochemical reactions for the synthesis of the higher alcohols contained in tequila as: Propanol, isobutanol, 2-Phenyl-ethanol, isoamyl and amyl alcohol; involving 94 metabolites and 117 reactions; of which 93 correspond to biochemical internal reactions and 24 to transport fluxes between the medium and the cell. The model is validated under aerobic and anaerobic conditions and applied for the first time to de fermentation of *Saccharomyces cerevisiae* in agave juice for tequila production using the Flux Balance Analysis (FBA)

 doi:10.20944/preprints201811.0385.v1

to estimate its metabolic fluxes. Flux Balance Analysis (FBA) has demonstrated to be a fundamental alternative to investigate the capacities of reconstructed metabolic networks due to the scarcity of information on the kinetic parameters associated with them [21]. Computational algorithms such as FBA, based on restrictions, are essential tools to predict the phenotypical properties in GSM, and these have been widely utilized in different model strains [13]. Genomic information coupled with biochemistry and specific information on the strains of the microorganisms have been utilized to reconstruct metabolic networks for sequenced organisms [22].

This information itself is not sufficient for completely specifying the expression of the metabolic phenotype under the different fermentation conditions. However, a microorganism's metabolic phenotype can be analyzed based on flux distributions in a metabolic network. The interpretation and prediction of metabolic flux distributions requires mathematical modeling and computerized simulation [22]; therefore, various methodologies have been developed to analysis the cellular metabolism and its regulation: one of these methodologies is the Flux Balance Analysis (FBA), which has been successfully applied in *Escherichia coli* and *S. cerevisiae* for determination of the fluxes of their cellular metabolism.

An important difference between fungi and bacteria is that bacteria tend to achieve greater product yields than the fungi, this is due in part to greater complexity and compartmentalization, in fungal metabolism. Likewise, the development of compartmentalized models for *S. cerevisiae* represents a greater challenge than those for *E. coli* [11]. Matsuda et al., (2011) realized simulations of a model of the central metabolism of *E. coli* and the *S. cerevisiae* where they found it was found a higher production yield of higher alcohols in *E. coli* which could be attributed to a greater degree of metabolic flexibility in comparison with that of *S. cerevisiae* [11].

Employing FBA methodology in *S. cerevisiae* metabolic network, it was found that the global cellular functions of the growth and secretion of metabolic products under aerobic and anaerobic culture were consistent with the experimental data [24]. Pereira et al., (2016) selected four of these GSM of *S. cerevisiae*: iFF708; IMM904; iTO977, and Yeast 6. They carried out simulations to find which of these exhibited best adjustments with respect to experimental fluxes *in vivo*. They found that the first model built, iFF708, showed the best predictions in terms of the metabolic flux distribution of the central metabolism.

For the effects of generating a GSM, that could serve in the future for developing a control system for the alcoholic fermentation process, it is necessary to generate a stoichiometric model with a less number of reactions which could be easy to use and to implement in an industrial process. Thus, ensuring the quality and productivity of the alcoholic fermentation phase for the production of tequila.

 doi:10.20944/preprints201811.0385.v1

Although, there are many studies on *S. cerevisiae* in the literature, to our knowledge there is no report up to date, regarding to the estimation of metabolic fluxes in *S. cerevisiae* for tequila production, and describing the flux distribution in higher alcohols.

While traditionally the tequila production is carried out in batch process, a recent alternative comprises the case of continuous cultures processes, which could be successfully utilized for studying the regulation of the glycolytic enzymes of *S. cerevisiae* under different fermentation conditions [3]. Therefore, in this research a stoichiometric model is re-constructed and it is validated using FBA with another model previously reported in the literature [24] and also employed to estimate metabolic flux distributions, based on experimental data of continuous fermentation of agave juice for tequila production reported in the literature [3].

2. Materials and Methods

2.1 Flux Balance Analysis

Flux Balance Analysis (FBA), is a methodology employed to analyze metabolic fluxes through a metabolic network [25]. FBA is a metabolic engineering tool that can be used for analyzing the capacities of a metabolic network reconstructed on systemic stoichiometry, thermodynamic restrictions and transport capacity of the biological system [22]. Subject to these restrictions, optimal flux distributions are calculated using lineal programming techniques. On base to the calculation and the analysis of optimal flux distributions under different conditions, it is possible to generate quantitative hypotheses *in silico* that can be tested experimentally [22].

2.1.1 Mathematical representation of FBA

From the biochemical information, the mathematical representation of the metabolic system, starts from a mass balance of each metabolite in the biological system, which is expressed as a matricial form Equation (1):

$$\frac{dX}{dt} = S.V. \qquad (1)$$

Where X [mmol/g D.W.] denotes the concentration vector of all metabolites considered in the metabolic network, S represents the stoichiometric matrix, and v [mmol/g D.W. h^{-1}], the internal flux vector and those exchange fluxes considered between the organism and the culture medium. Under steady-state conditions that above equation become as Equation (2):

$$S.V = 0. \qquad (2)$$

Thus, the mathematical representation is a system of linear homogeneous equations, which is a sub-determined system; it is because the number of reactions normally exceeds the number of metabolites. This system of equations is resolved by applying the linear programming technique, maximizing an objective function that is commonly the growth of the microorganism, which has been experimentally corroborated [22].

 doi:10.20944/preprints201811.0385.v1

The objective function of growth Z is defined by the microorganism's biomass and it is expressed mathematically by means of the Equation (3):

$$z = \sum_{m=1}^{M\,Vgrowth} d_m \cdot x_m \rightarrow Biomass \qquad (3).$$

Where d_m is the proportion of each metabolite X_m, in the composition of the biomass. Applying thermodynamic restrictions (4), and those interchange fluxes related with the transport capacities (5), where α_j and β_j comprise the scalar data that determine transport capacity and biological system exchange. On base to the above equations the optimal flow distribution is determined in the metabolic network.

$$V_j \geq 0. \qquad (4).$$

$$\alpha_j \leq b_j \leq \beta_j \qquad (5).$$

2.1.2 *Construction of the Stoichiometric Model*

The model developed was built based on the stoichiometric model for *S. cerevisiae* reported in the literature [26], which is an aerobic model applied to an alcoholic fermentation process under continuous culture with minimal medium and it was utilized for the metabolic-flux calculation employing Metabolic Flux Analysis (MFA) methodology.

Taken as base the referred model it is considered of the central metabolism of *S. cerevisiae*, the glycolysis (reactions 1–8), and the fermentative pathways for the production of acetate, glycerol, and ethanol (reactions 9, 10, 11, 12, 15, and 16) under anaerobic conditions. The pentose phosphate pathway (reactions 17–22) and the Krebs cycle (reactions 23–31) were taken from an anaerobic aerobic stoichiometric model reported in the literature [27]. For production of the acetate and ethanol metabolites, it is added two reactions (reactions 13 and 14), which are considered in the model reported in the literature [28].

2.1.3 *Growth objective Function*

The objective function of the growth is defined on base to the biomass composition of *S. cerevisiae*. It is represented by the flux (reaction 65), which considers the composition of its macromolecules: proteins; carbohydrates; lipids; Deoxy-ribonucleic acid (DNA), and Ribonucleic acid (RNA) [26].

For fermentations under continuous culture, the cellular composition of biomass varies according to the Dilution rate (D)[h^{-1}]. The most important variation in biomass composition is found in proteins and in RNA, which increase linearly according to the D rate (Table 1) and at the expense of the carbohydrates [26]. For the optimizations carried out in the present article, it is took as reference the biomass composition corresponding to D = 0.1 h^{-1}.

 doi:10.20944/preprints201811.0385.v1

Table 1. Composition of the biomass (Nissen et al., 1997)

METABOLITE	CELLULAR CONTENT (% weight)			
	D = 0.10 h^{-1}	D = 0.20 h^{-1}	D = 0.30 h^{-1}	D = 0.40 h^{-1}
Protein	45.0	50.0	55.5	60.1
Glycogen	8.4	4.2	0.6	0.0
Trehalose	0.8	0.2	0.0	0.0
Mannose	13.1	12.9	12.0	13.3
Other carbohydrates	18.4	15.4	12.6	3.7
RNA	6.3	8.2	10.1	12.1
DNA	0.4	0.4	0.5	0.6
Free amino acids	1.1	1.3	1.1	2.0
Lipids	2.9	3.0	3.8	3.4
Ashes	5.0	5.0	5.0	5.0
Total	101.4	100.6	101.2	100.2

D = Dilution rate. [h^{-1}]

This model was built with the purpose of operating under anaerobic as well as under aerobic conditions. Reactions (14, 12, 16, 26, and 33) would operate only under aerobic conditions, while reactions (15, 13, and 27) would operate only under anaerobic conditions.

For synthesis of the different macromolecules present in *S. cerevisiae*, the polymerization energy reported in the literature was considered in the reaction (65) [14].

2.1.4 Biochemical Protein Synthesis

Protein synthesis (reaction 63) considers the 20 amino acids, 15 of them are represented by only one reaction for each amino acid (reactions 35–49), from their growth precursors and from the metabolic costs reported in the literature [29].

In the specific case for the synthesis of amino acids leucine (LEU), valine (VAL), threonine (THR), isoleucine (ILEU), and phenylalanine (PHE), reactions (reactions 80–91) are taken from those reported in the literature [30), which are considered in two reactions: the first one, consists of the amino acid precursor towards the formation of α-keto acid, and the second one, from the α-keto acid produced towards the corresponding amino acid. These amino acids are related with the synthesis of the higher alcohols. Furthermore, the amino acids constitute a nitrogen source present in the complex medium, such as in the case of the agave juice utilized for tequila production, which contains dissolved amino acids that could be assimilated as the nitrogen source.

2.1.5 Higher-alcohol synthesis

The synthesis of higher alcohols is linked with the amino acids through α-keto acids, which are precursors of n-Propanol, Isoamyl and amyl alcohol; 2-Phenyl-ethanol, and isobutanol. Production of higher alcohols (reactions 70–79), can be represented by the following two pathways[30]:

1. The catabolic pathway (Ehrlich pathway), which involves transamination and deamination of the amino acids in the culture medium (reactions 81-92).

 doi:10.20944/preprints201811.0385.v1

2. The anabolic pathway, which permits synthesis of the α-keto acid acids from the sugars present in the medium. From the α-keto acid, the higher alcohol is obtained that corresponds to the same mechanism as that of the catabolic pathway (reactions 71-80).

2.1.6 Synthesis of RNA and DNA

For the synthesis of macromolecules of RNA (reaction 65) and DNA (reaction 66), they include the formation of molecules for the biosynthesis of their nucleotides, for RNA from adenosine-monophosphate (AMP), Guanosine-monophosphate (GMP), Cytidine-monophosphate (CMP), and Uridine-monophosphate (UMP) (reactions 50–53), and for DNA, from deoxyadenosine monophosphate (dAMP), deoxyguanosine monophosphate (dGMP), deoxycytidine monophosphate (dCMP), and deoxyuracil monophosphate (dUMP) (reactions 54–57) [29].

2.1.7 Synthesis of carbohydrates

The composition of carbohydrates for *S. cerevisiae* includes glycogen, trehalose, mannose, and other carbohydrates, according to those reactions reported in the literature [26,27,28], which are considered in reaction 64.

2.1.8 Synthesis of lipids

The lipids of *S. cerevisiae* are composed mainly of phospholipids, sterols, and triacylglycerols, whose compositions are 54, 3, and 20% respectively. The main building blocks for synthesis of lipids comprise the fatty acids, where the palmitic, oleic, and linoleic fatty acids, represent the 75% of abundance [29]. With respect to the phospholipids composition in *S. cerevisiae*, it is understood that phosphatidylcholine, phosphatidylethanolamine, and phosphatidylinositol represent > 90%. With regard to the composition of sterols in *S. cerevisiae*, ergosterol is the most abundant, and it represents 90%. Therefore, the lipid synthesis (reaction 67) was proposed based on [29].

2.1.9 Oxidative Phosphorylation

In order for the model to be able to work under aerobic conditions, the oxidative phosphorylation (reactions 32, 33, and 34) is included. From previous models of *S. cerevisiae* reported in the literature [27,28], the stoichiometric ratio of oxidative phosphorylation of P/O = 1.0. was considered.

2.1.10 Cellular maintenance

Cellular maintenance (reaction 69) takes into account the consumption of the Adenosine triphosphate (ATP) utilized in cell-repair functions. In *S. cerevisiae*, it is known that cellular maintenance is <1 mmol ATP/g Dry Weight (DW) [29], considering that in the present article, the exact value of 0.7 mmol ATP/g DW was employed for conducting the different scenarios.

2.1.11 Description of the model

In the present work, the stoichiometric model built comprises 117 reactions and 93 metabolites. From the 117 reactions considered, 93 correspond to internal reactions and 24 to transport or exchange fluxes between the external environment and the cell. The exchange fluxes considered were the following metabolites: glucose; fructose; ammonium; glutamine(GLN); LEU, ILEU, VAL, THR,

 doi:10.20944/preprints201811.0385.v1

and PHE; oxygen; sulfate; carbon dioxide (CO2); propanol; isobutanol; isoamyl; amyl; phenylethanol; ethyl acetate; ethanol; glycerol; acetate; acetaldehyde; succinate, and biomass.

2.1.12 Compartmentalization

Compartmentalization was carried out for the compounds OAA, ACCOA, NADH, and NADPH, which participate in reactions in the mitochondria as well as in the cytosol [26].

3. Results

3.1. Validation of the Stoichiometric Model

The stoichiometric model constructed was validated under fermentation conditions (anaerobic) and under growth conditions (aerobic), comparing it with models reported in the literature [15,26]. For conducting simulation *in silico*, cellular maintenance (m) was considered as m = 0.7, as well as a Molecular Weight (MW) for the biomass of 28 g/C-mol [26].

3.1.1. Validation of the Stoichiometric Model Under Anaerobic Conditions

To validate the reconstructed model under anaerobic conditions, the flux for the consumption of glucose at D = 0.1 h^{-1} was calculated utilizing the Pirt maintenance model [26]. This flux of Glucose correspond to 5.917 mmol/g DW h and it was established as experimental restriction equation (5). For oxygen, its flux was zero as it is an anaerobic condition; ammonium was considered as an unique nitrogen source without any restriction (Table 2).

Table 2. Experimental restrictions specified in optimization under anaerobic conditions

Metabolite	Li (mmol/g DW h)	Ls (mmol/g DW h)
Glucose	0	5.917
Oxygen	0	0
Ammonium	0	1,000

DW = Dry Weight. Li=inferior limit, Ls=superior limit.

The results were compared with another data *in silico* reported in the literature. The major products of the fermentation (ethanol, biomass, and CO_2) presented a good deviation of 2.41, 0.9, and 2.6%, and glycerol (Table 3), 21% with respect to the values predicted by [26]. The non-production of acetate is due to that the program calculates optimal solutions [24].

Preprints (www.preprints.org) | NOT PEER-REVIEWED | Posted: 16 November 2018 doi:10.20944/preprints201811.0385.v1

Table 3. Theoretical yields obtained with the model proposed during fermentation

D = 0.1 h^{-1}	This study		Nissen et al., (1997)
m = 0.7 Metabolite	Molar flux mmol/(g DW h)	Yields C-mol/C-mol glucose	Yields C-mol/C-mol glucose
Ethanol	9.133	0.514	0.497
Glycerol	1.082	0.0914	0.086
Biomass	0.106	0.106	0.107
CO2	9.72	0.274	0.272
Succinate	0.000	0.000	0.003
Acetic	0.000	0.000	0.002
Pyruvic	0.000	0.000	0.001
Total	-------	0.985	0.968

D = Dilution Rate [h^{-1}].

3.1.2. Validation of the Stoichiometric Model Under Aerobic Conditions

For the aerobic conditions, the model was tested under three conditions with the following different oxygen consumptions: microaerobic fermentation; oxido-fermentative growth, and aerobic growth.

3.1.2.1. a) Microaerobic fermentation

In the simulation of the microaerobic fermentation the restrictions were considered as follows: glucose consumption flux of 14 mmol/g DW h, and oxygen consumption flux of 1 mmol/g DW h. Ammonium was considered as sole nitrogen source and without restriction in terms of its transport or consumption (Table 4).

Table 4. Experimental restrictions specified in optimization under microaerobic conditions

Metabolite	Li (mmol/g DW h)	Ls (mmol/g DW h)
Glucose	0.00	14.00
Oxygen	0.00	1.00
Ammonium	0.00	1,000

Li: inferior limit of flux, Ls: Up Limit of flux.

Simulation of microaerobic fermentation (Table 5) predicted a growth-specific velocity value (μ) of 0.324 mmol/g DW h, which represents 1.8% less than the value estimated *in silico* and 4.5% greater than that of the experimental value determined in the literature [15].

With respect to the ethanol flux, this was 21.01 mmol/g DW h, representing 1.31% less than that reported in the literature [15] obtained *in silico* and 4.63% deviation with regard to that reported experimentally in the same article.

It is observed that for microaerobic fermentation (Table 5), the values determined for μ present a deviation of 2.42% less with respect to those obtained *in silico* and of 3.87% more in relation to the experimental value.

Preprints (www.preprints.org) | NOT PEER-REVIEWED | Posted: 16 November 2018 doi:10.20944/preprints201811.0385.v1

Table 5. *Comparison of predictions in silico in microaerobic fermentation*

Microaerobic fermentation			
	Oxygen 1 mmol/(g DW h) Glucose 14 mmol/(g DW h)		
m = 6			
	This study	**Duarte *et al.* (2004)**	
	mmol/g DW h		
		In silico	Experimental
μ	0.322	0.33	0.31
Ethanol	21.01	21.29	20.08
Acetate	0.00	0.26	0.22

DW = Dry Weight.

3.1.2.2. b) Oxido-fermentative growth

Simulation *in silico* of oxido-fermentive growth was carried out considering the following restrictions: glucose consumption velocity of 12 mmol/g DW h; maximal oxygen consumption velocity of 9 mmol/g DW h, and again, ammonium as the source of nitrogen velocity of 1 mmol/g DW h (Table 6).

Table 6. Experimental restrictions specified in optimization under oxido-fermentative growth

Metabolite	**Li (mmol/g DW h)**	**Ls (mmol/g DW h)**
Glucose	0.00	12.00
Oxygen	0.00	9.00
Ammonium	0.00	1,000

The previous simulation gave a growth-specific velocity value (μ) of 0.51 h^{-1}, which represents 3.77% less than the value estimated *in silico* (Table 7) and the same as that determined experimentally and reported in the literature [15]. Regarding the ethanol flux, it was obtained as 14.03 mmol/g DW h. This presented 17.11% of variation with respect to that obtained *in silico* [15] and 21.10% deviation with respect to that value determined experimentally in the same source already cited.

In the case of the acetate, our model did not predict any flux. The above could be due to the less number of reactions considered in the model [15]. This behavior has been also reported in model with a greater number of reactions [24]. It could be also due to the fact that the optimization carried out was directed toward maximizing biomass production, in which acetate production tends to diminish the value of our growth-objective function.

Table 7. Comparison of predictions *in silico* under oxido-fermentative growth

	Oxido-fermentative growth		
m = 0.7	**Oxygen 9 mmol/(g DW h)**	**Glucose 12 mmol/(g DW h)**	
	This study mmol/(g DW h)	**Duarte et al. (2004)**	
		In silico	Experimental
μ	0.51	0.53	0.51
Ethanol	14.03	11.98	11.07
Acetate	0.00	2.62	2.57

 doi:10.20944/preprints201811.0385.v1

DW = Dry Weight.

3.1.2.3. c) Glucose-limited Aerobic Growth

For simulation of glucose-limited aerobic growth, the following restrictions (Table 8) were applied: glucose consumption velocity of 2.5 mmol/g DW h; maximal oxygen consumption velocity of 8 mmol/g DW h, and, once again, ammonium as the sole nitrogen source.

Table 8. Experimental restrictions specified in optimization under Glucose-limited Aerobic Growth

Metabolite	Li (mmol/g DW h)	Ls (mmol/g DW h)
Glucose	0.00	2.50
Oxygen	0.00	8.00
Ammonium	0.00	1,000

The results of the simulation (Table 9) exhibit a μ value of 0.20 h^{-1}, which represents 9.09% less than the value estimated *in silico* and one similar to that determined experimentally in the literature [15].

Table 9. Comparison of predictions *in silico* in glucose-limited aerobic growth

	Glucose-limited aerobic growth		
	Oxygen 8 mmol/(g DW h)	**Glucose 2.5 mmol/(g DW h)**	
m = 0.7			
	This study (mmol/g DW h)	**Duarte *et al.* (2004)**	
		In silico	**Experimental**
μ	0.20	0.22	0.20
Ethanol	0.00	0.00	0.16
Acetate	0.00	0.00	0.31

DW = Dry Weight.

Additionally, it was found that the oxygen flux consumption required in the model was 7.07 mmol/(g DW h). Regarding the 8 mmol/(g DW h) in the *in silico* study, this difference can be due to the following: That the reactions number considered is different in our model. A total of 127 reactions were considered, while in the model in the literature [15], 1,200 reactions were considered. That the composition of the biomass was different at a Dilution (D) rate of 0.05 h^{-1}. Once time the model was tested and with good results then we study the effect of dilution rate during fermentation by *S. cerevisiae* of agave juice.

3.2. Simulation in Silico of agave-Juice fermentations under continuous culture for Tequila production: effect of the dilution rate.

From the experimental data reported in the literature [3] regarding continuous agave-juice fermentations, the authors calculated experimental fluxes for fructose consumption, ethanol production, and specific growth velocity, and they used the production fluxes of the volatile compounds to study the effect of the dilution rate in metabolism of *S. cerevisiae* during continuous fermentation of agave juice for tequila production.

Morán et al., (2011) studied the effect of the Dilution (D) rate in a continuous culture fermentation of *S. cerevisiae* in agave-juice during tequila production. Results are shown at Table 7. From this set of

 doi:10.20944/preprints201811.0385.v1

experimental values, the fluxes of sugar (Fructose and glucose), ethanol and the specific growth velocity were estimated (see Table 10). Additionally, the fluxes of volatile compounds were also estimated.

Table 10. Metabolic fluxes deriving from experimental data of fermentation with agave juice at different Dilution (D) rates

D1 (h^{-1})	Biomass1 (g/L)	Ethanol1 (g/L)	Residual1 Sugars (g/L)	Rx1 (g/L h)	Rp1 (g/L h)	Rs1 (g/L h)	Sugar flux (mmol/g DW h)	Ethanol flux (mmol/g DW h	Specific Growth velocity (μ) (h^{-1})
0.04	5.83	43.92	3.94	0.23	1.76	3.80	3.671	6.654	0.04
0.08	3.38	29.63	35.34	0.27	2.37	5.08	8.362	15.266	0.08
0.12	3.04	19.76	59.75	0.36	2.37	4.69	8.685	17.174	0.12
0.16	2.75	9.95	79.08	0.44	1.59	2.52	5.092	12.569	0.16

Experimental Data of Source: (3).
Rx, Rp, and Rs represent productivity of biomass, ethanol and sugars of the fermentation process.

The above estimated fluxes were employed as restrictions in our model for carrying out simulations *in silico* and for estimating the distribution of metabolic fluxes (Fig. 1, Fig. 2 and Fig. 3). Optimization was performed under anaerobic conditions, restricting oxygen consumption flux with a value of zero, and considering as a restriction a maximal limit of the ammonium phosphate consumption flux as nitrogen source. Higher-alcohol production fluxes were indicated as experimental restrictions.

From the fluxes calculated *in silico* (Table 11), it was found that the model predicts an ethanol flux of 5.8 mmol/g DW h, which presents a deviation of –13% with respect to that value calculated from the experimental data of 6.654 mmol/g DW h. The specific growth velocity (μ) was established in the optimization at 0.04 h-1, which corresponds to the fermentor's continuous dilution rate of D = 0.04 h^{-1}. The cellular maintenance considered was 0.7 mmol ATP/g DW h which is the value reported for *S. cerevisiae* [29].

Preprints (www.preprints.org) | NOT PEER-REVIEWED | Posted: 16 November 2018 doi:10.20944/preprints201811.0385.v1

Table 11. Estimation of metabolic fluxes based on experimental fluxes Dilution (D) = 0.04 h^{-1}

FLUXES	D = 0.04 h^{-1} *Experimental (mmol/g DW h)	*In silico* (mmol/g DW h)	% Variation
Fructose	3.671	3.671	0%
Ethanol	6.654	5.8	-13%
Biomass	0.04	0.04	0%
CO2		7.448	
Nitrogen source (ammonium)		0.274	
Acetaldehyde	0.0036	0.0035	0%
Methanol	0.0373		
n-Propanol	0.0066	0.0066	0%
Isobutanol	0.0017	0.0017	0%
Isoamyl and amyl alcohol	0.0092	0.0092	0%
2-Phenyl-ethanol	0.00059	0.00059	0%
Ethyl acetate	0.00063	0.00063	0%

Similarly, *in silico* optimizations using FBA were conducted for the remaining dilution rates (D = 0.04 h^{-1}, D = 0.08 h^{-1}, D = 0.12 h^{-1}, D = 0.16 h^{-1}), obtaining a good adjustment regarding ethanol flux, see Table 9. However, the adjustment diminished as the dilution rate increased. For the case of D=0.16 h^{-1} it was not possible to obtain a map of fluxes distribution with the flux of sugar established in Table 12.

Table 12. Estimation of ethanol flux based on experimental fluxes for different dilution rates

Volatile compounds	D=0.04 (h^{-1})	D=0.08 (h^{-1})	D=0.12 (h^{-1})	D=0.16 (h^{-1})
	mmol/D.W. h	mmol/D.W. h	mmol/D.W. h	mmol/D.W. h
Experimental ethanol	6.6541	15.266	17.174	12.569
Glycerol	0.433	2.7138	1.2808	1.185
Acetaldehyde	0.00355	0.01350	0.02843	0.02617
Methanol	0.03728	0.08933	0.15275	0.15163
n-Propanol	0.00656	0.01332	0.01628	0.01269
Isobutanol	0.00170	0.00454	0.00611	0.00543
Isoamyl and amyl alcohol	0.00919	0.01137	0.01377	0.01018
2-Phenyl-ethanol	0.00059	0.00235	0.00344	0.00492
Ethyl acetate	0.00063	0.00116	0.00229	0.00155

4. Discussion

In the flux distribution map under continuous culture, it is possible to identify activation of different pathways of metabolism of *Saccharomyces cerevisiae*: glycolysis, pentoses phosphate,

fermentative pathways, cycle of Krebs, oxidative, phosphorylation and the fluxes of consume or production or metabolites (Fig. 1, Fig. 2 and Fig. 3).

It is possible to appreciate the variation discussed by [3] where they affirm that when the dilution rate increases in the range from D=0.04 to D=0.08 h^{-1}, exist an increase of the fluxes of: production of glycerol and acetaldehyde as well as an increment in the consume of ammonium.; while, exist a decrement of production of higher alcohols (Table 13). This phenomenon is attributed to exist an inverse relation between ammonium consume and the production of higher alcohols. Regularly, in some fermentations a high consume of ammonium is correlationated with a high synthesis of glycerol, acetate and acetaldehyde, but with a diminution of synthesis of higher alcohols [31].

Table 13. Estimation of fluxes of ethanol, Glycerol, acetaldehyde and volatile compounds for different dilution rates

Ethanol flux			
	***Experimental (mmol/g DW h)**	***In silico* (mmol/g DW h)**	**% Variation**
D = 0.04 h^{-1}	6.6541	5.813	-13%
D = 0.08 h^{-1}	15.266	11.469	-24%
D = 0.12 h^{-1}	17.174	13.155	-23%
D= 0.16 h^{-1}	12.569	-	-

The above results are represented with the flux distribution maps (Fig. 1, Fig. 2 and Fig. 3). Agree with the our study this scenario is explained as following: if the dilution rate increase, *Saccharomyces cerevisiae* requires an higher level of nitrogen source, but due to the fact that the nitrogen source is limited then is very probable that the regulation of the pathway influence in reduce the anabolic pathways of biosynthesis of aminoacids and then increase the synthesis of higher alcohol is produced via anabolic route from aminoacids (LEU, ILEU, VAL, THR and PHE) presents in the agave juice [6]. Moran et al., (2011) found than when the dilution rate increases (D), the efficiency of the fermentation is reduced, then decrease the concentration of biomass, ethanol and higher alcohols while the residual sugar concentration increase.

The three states physiological states are estimating and they are shown in the map of fluxes distribution from experimental results of fermentation reported in literature:

a) Map One (D=0.04 h^{-1}), Represent the highest concentration of alcohol and higher alcohols (Fig. 1).

This physiological state has the highest fermentative capacity of the four states explorated by Moran y col., 2011. Because it has the highest concentration of alcohol (43.92 g/L) and has the highest concentration in higher alcohol. As well as the highest concentration of biomass (5.83 g/L) and attain the minimum residual sugar concentration in the fermentation media (3.94 g/L) consuming practically all the sugar present. The productivity of alcohol reach the second place with a value of (1.76 g/L h) in comparison with the others three dilution rates (Tabla 1).

b) Map two (D=0.08 h^{-1}), Represent the maximum sugar consumption rate (Fig. 2).

This physiological state is interesting because it is one of two that has the highest productivity of alcohol (2.37 g/L h) similar to dilution rate D = 0.12 h^{-1} in comparison with the others two dilution rates. This has the maximum sugar consumption (5.08 g/L h) and the second in concentration of

Preprints (www.preprints.org) | NOT PEER-REVIEWED | Posted: 16 November 2018 doi:10.20944/preprints201811.0385.v1

alcohol (29.63 g/L), and second in the concentration of residual sugar in the media (35.34 g/L) and second in the biomass concentration (3.38 g/L).

c) Map three (D=0.12 h^{-1}), Represent the highest ethanol production (Fig. 3).

This physiological state is one of two that has the highest productivity of alcohol (2.37 g/L h) similar to dilution rate D = 0.08 h^{-1} in comparison with the others two dilution rates.

This has the second place in sugar consumption rate (4.69 g/L h) and the third place in concentration of alcohol (19.76 g/L), and third place in the concentration of residual sugar in the media (59.75 g/L) and the third place in the biomass concentration (3.04 g/L).

In this state the flux of production of ethanol (mmol/D.W h) is the highest due to the biomass concentrations are very similar between the four states and the flux is calculated in function of biomass concentration in dry weight.

The dilution rate (D=0.08 h^{-1} -0.16 h^{-1}) shown a low fermentative capacity which could be due to a low content of nutrients in agave juice [32]. While D increase in the range of D=0.04 h^{-1} to D=0.12 h^{-1}, the concentrations of higher alcohols (n-propanol, iso-butanol, isobutyl alcohol, amyl and isoamyl alcohol, and 2-Phenyl-ethanol) decreased moreover their fluxes of production shown in the map of fluxes distribution of this compounds (Fig. 1, Fig. 2 and Fig. 3) increase due to the effect of the diminution of biomass concentration and the increase of dilution rate, which are used to calculate this.

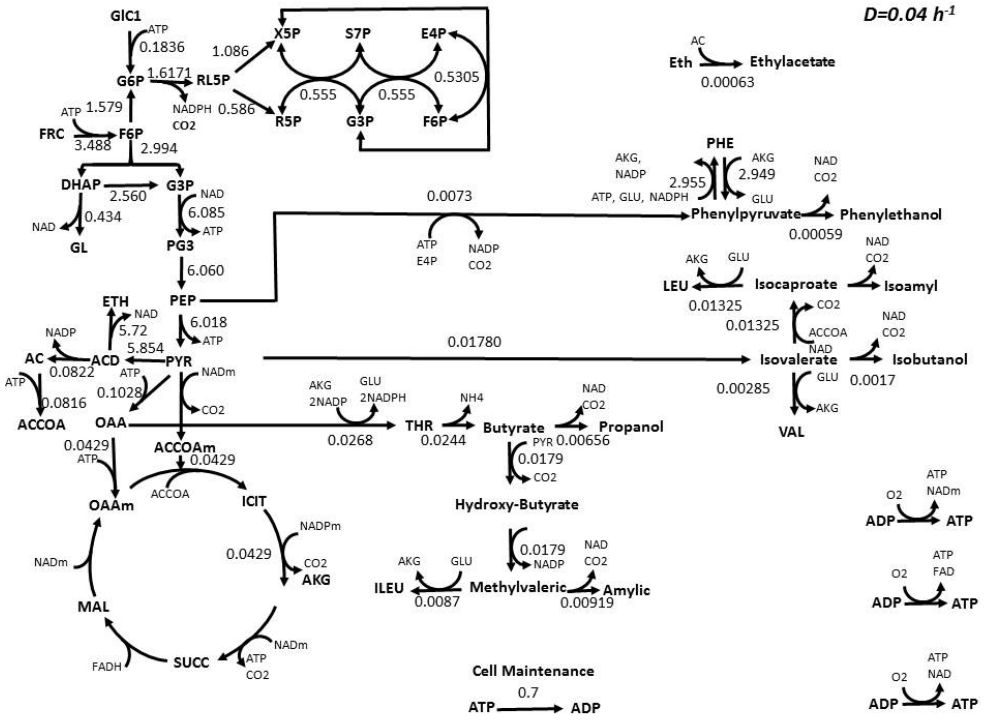

GLC	0.1835
FRUC	3.488
NH4	0.2780
GLN	0
VAL	0
LEU	0
ILEU	0
THR	0
PHE	0
O2	0
SO4	0.0093
CO2	7.519
Propanol	0.00656
Isobutanol	0.0017
Isoamylic	0.0
Amylic	0.00919
Phenylethanol	0.00059
Ethylacetate	0.00063
Ethanol	5.767
Glycerol	0.433
Succinate	0
Acetaldehyde	0.00355
Biomass	0.04

Figure 1. Central metabolism flux distribution and higher alcohol fermentations of agave juice under continuous culture with *Saccharomyces cerevisiae* D=0.04 h^{-1}.

 doi:10.20944/preprints201811.0385.v1

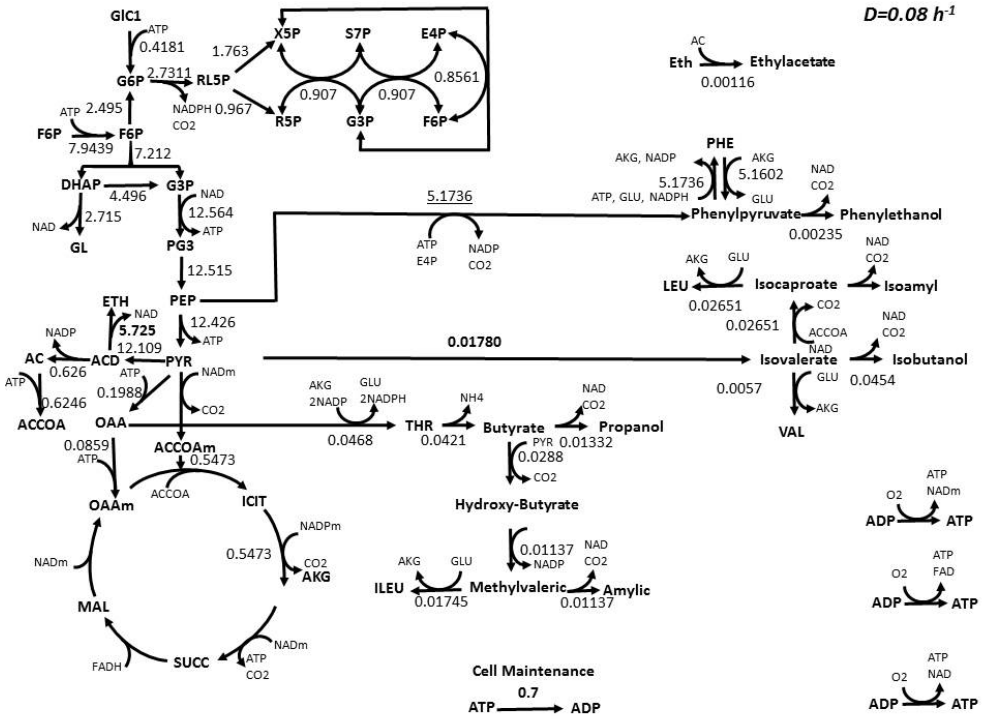

GLC	0.4181
FRUC	7.9439
NH4	0.5562
GLN	0
VAL	0
LEU	0
ILEU	0
THR	0
PHE	0
O2	0
SO4	0.0187
CO2	15.7488
Propanol	0.01332
Isobutanol	0.00454
Isoamylic	0.0
Amylic	0.01137
Phenylethanol	0.00235
Ethylacetate	0.00116
Ethanol	11.469
Glycerol	2.7138
Succinate	0
Acetaldehyde	0.0135
Biomass	0.08

Figure 2. Central metabolism flux distribution and higher alcohol fermentations of agave juice under continuous culture with *Saccharomyces cerevisiae* D=0.08 h^{-1}.

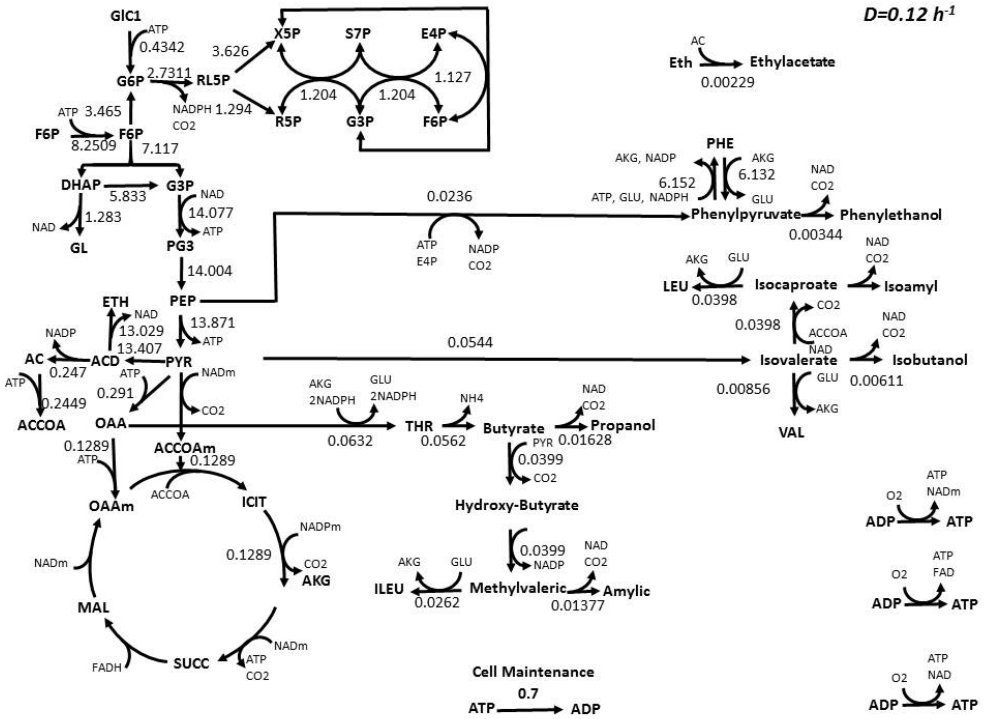

GLC	0.4342
FRUC	8.2509
NH4	0.834
GLN	0
VAL	0
LEU	0
ILEU	0
THR	0
PHE	0
O2	0
SO4	0.0187
CO2	17.0066
Propanol	0.01628
Isobutanol	0.00611
Isoamylic	0.0
Amylic	0.01377
Phenylethanol	0.00344
Ethylacetate	0.00229
Ethanol	13.155
Glycerol	1.2808
Succinate	0
Acetaldehyde	0.00248
Biomass	0.12

Figure 3. Central metabolism flux distribution and higher alcohol fermentations of agave juice under continuous culture with *Saccharomyces cerevisiae* D=0.12 h^{-1}.

The contribution of the model developed lies in that it serves as a platform for the study of the metabolism of the assimilation of nitrogen in yeast. This is because it is considered that nitrogen

metabolism, including the synthesis and transport pathways for each of the amino acids, in that the latter these can function as nitrogen source, in addition to the fact that the Ehrlich pathway for higher-alcohol synthesis, is associated with the amino-acid pathways, given that their higher-alcohol production takes place through the decarboxylation medium via α-ketoacids, followed by a reduction of the aldehyde of the corresponding alcohol. Keto acids are produced by two pathways: the catabolic pathway from the amino acids of the culture medium, or the anabolic pathway by means of the sugars of the medium [33].

5. Conclusions

Here we show for first time the different physiological states represented by the map of distributions of fluxes for tequila production by fermentation of continuous culture reported in literature [3].

The model built was validated satisfactorily under anaerobic and aerobic conditions and predicts the flux values of the principal metabolites associated with fermentation, in relation to the data calculated *in silico* and the experimental data reported in the literature.

The model developed constitutes a tool for the estimation of flux distribution maps during fermentation processes for the production of tequila, in which it is possible to visualize the central metabolism and the synthesis pathways of the higher alcohols.

The stoichiometric model developed in the present article and based on experimental fluxes (fructose and biomass) allowed to obtain an estimate of the metabolic flux distribution of *Saccharomyces cerevisiae* associated to physiological states of the yeast during the fermentation in continuous agave-juice fermentation for tequila production.

Author Contributions: Conceptualization, O.G.R and J.D.P.R.; methodology O.G.R and J.D.P.R.; validation, O.G.R and J.D.P.R.; formal analysis, O.G.R and J.D.P.R.; investigation, O.G.R and J.D.P.R.; writing—original draft preparation, J.D.P.R.; writing—review and editing, O.G.R and J.D.P.R., A.G.M.; visualization, A.G.G.

Funding: This research received no external funding.

Acknowledgments: To Consejo Nacional de Ciencia y Tecnología (CONACYT) for the fellowship granted (fellowship number: 174828 and registry number: 165004) and to CIATEJ and UdeG for the facilities and support during the development of the present work.

Conflicts of Interest: "The authors declare no conflict of interest."

Appendix A

Reactions list of stoichiometric model.

References

1. "NOM-006-SCFI-2012," *Norma Oficial Mexicana NOM-006-SCFI-2012*. Bebidas Alcohólicas-Tequila-Especificaciones. Secretaría de Comercio y Fomento industrial. Diario Oficial de la federación. México DF. 13 de Diciembre del 2012.

2. Cedeño M.C.; Tequila Production. *Crit Rev Biotechnol* **1995**, 15(1):1–11, https://doi.org/10.3109/07388559509150529.

3. Morán-Marroquín G.A.; Córdova J.; Valle-Rodríguez J.O.; Estarrón-Espinosa M., Díaz-Montaño D.M. Effect of dilution rate and nutrients addition on the fermentative capability and synthesis of aromatic compounds of two indigenous strains of *Saccharomyces cerevisiae* in continuous cultures fed with Agave tequilana juice. *Journal of the Science of Food and Agriculture* **2011**, 151(1):87–92, https://app.dimensions.ai/details/publication/pub.1010598182.

4. Benn S.M.; Peppard T.L. Characterization of Tequila Flavor by Instrumental and Sensory Analysis. *J Agric Food Chem* **1996**, 44(2):557–66, https://doi.org/10.1021/jf9504172.

5. Pinal L.; Cedeño M.; Gutiérrez H.; Alvarez-Jacobs J. Fermentation parameters influencing higher alcohol production in the tequila process, *Biotechnol Lett* **1997**, 19(1):45–7, https://doi.org/10.1023/A:1018362919846.

6. Segura-García L.E., Taillandier P., Brandam C., Gschaedler A. Fermentative capacity of *Saccharomyces* and non-*Saccharomyces* in agave juice and semi-synthetic medium. LWT - *Food Sci Technol* **2015**, 60(1):284-291, http://www.sciencedirect.com/science/article/pii/S0023643814004939.

7. Pereira R.; Nielsen J.; Rocha I. Improving the flux distributions simulated with genome-scale metabolic models of *Saccharomyces cerevisiae*. *Metab Eng Commun* **2016**, 3:153–63. http://www.sciencedirect.com/science/article/pii/S2214030116300141.

8. Gombert A.K.; Moreira dos Santos M.; Christensen B.; Nielsen J. Network Identification and Flux Quantification in the Central Metabolism of *Saccharomyces cerevisiae* under Different Conditions of Glucose Repression. *J Bacteriol* **2001,** 183(4):1441-1451. http://jb.asm.org/content/183/4/1441.abstract.

9. Nilsson A.; Mardinoglu A.; Nielsen J. Predicting growth of the healthy infant using a genome scale metabolic model. *npj Syst Biol Appl* **2017**, 3(1):3.

https://doi.org/10.1038/s41540-017-0004-5.

10. Mardinoglu A.; Nielsen J. New paradigms for metabolic modeling of human cells. *Curr Opin Biotechnol* **2015**, 34:91–7. http://www.sciencedirect.com/science/article/pii/S0958166914002286.

11. Nielsen J.C.; Nielsen J. Development of fungal cell factories for the production of secondary metabolites:Linking genomics and metabolism. *Synth Syst Biotechnol* **2017**, 2(1):5–12. http://www.sciencedirect.com/science/article/pii/S2405805X17300066.

12. Monk J.; Nogales J.; Palsson B.O. Optimizing genome-scale network reconstructions. *Nat Biotechnol* **2014**, 32:447. https://doi.org/10.1038/nbt.2870.

13. Liu R.; Bassalo M. C.; Zeitoun R.I.; Gill R.T. Genome scale engineering techniques for

metabolic engineering. *Metab Eng* **2015**, 32:143–54. http://www.sciencedirect.com/science/article/pii/S1096717615001238.

14. Förster J.; Famili I.; Fu P.; Palsson B.Ø.; Nielsen J. Genome-scale reconstruction of the *Saccharomyces cerevisiae* metabolic network. *Genome Res* **2003**, 13(2):244–253. https://www.ncbi.nlm.nih.gov/pubmed/12566402.

15. Duarte N.C.; Palsson B.Ø.; Fu P. Integrated analysis of metabolic phenotypes in *Saccharomyces cerevisiae. BMC Genomics* **2004**, 5(1):63. https://doi.org/10.1186/1471-2164-5-63.

16. Kuepfer L.; Sauer U.; Blank L. M.; Metabolic functions of duplicate genes in *Saccharomyces cerevisiae. Genome Res* **2005**, 15(10):1421–30. https://www.ncbi.nlm.nih.gov/pubmed/16204195.

17. Nookaew I.; Jewett M.C.; Meechai A.; Thammarongtham C.; Laoteng K.; Cheevadhanarak S., et al. The genome-scale metabolic model iIN800 of *Saccharomyces cerevisiae* and its validation: a scaffold to query lipid metabolism. *BMC Syst Biol* **2008,** 2:71. https://www.ncbi.nlm.nih.gov/pubmed/18687109.

18. Mo M.L.; Palsson B.Ø.; Herrgård M.J. Connecting extracellular metabolomic measurements to intracellular flux states in yeast. *BMC Syst Biol* **2009,** 3(1):37. https://doi.org/10.1186/1752-0509-3-37.

19. Österlund T.; Nookaew I.; Bordel S.; Nielsen J.; Mapping condition-dependent regulation of metabolism in yeast through genome-scale modeling. *BMC Syst Biol* **2013,** 7(1):36. https://doi.org/10.1186/1752-0509-7-36.

20. Heavner BD, Smallbone K, Price ND, Walker LP. Version 6 of the consensus yeast metabolic network refines biochemical coverage and improves model performance. *Database (Oxford)* **2013,** 2013:bat059-bat059. https://www.ncbi.nlm.nih.gov/pubmed/23935056.

21. Vivek-Ananth R.P.; Samal A. Advances in the integration of transcriptional regulatory information into genome-scale metabolic models. *Biosystems* **2016,** 147:1–10. http://www.sciencedirect.com/science/article/pii/S0303264716300764.

22. Edwards J.S.; Covert M.; Palsson B. Metabolic modelling of microbes: the flux-balance approach. *Environ Microbiol* **2002**, 4(3):133–140. https://doi.org/10.1046/j.1462-2920.2002.00282.x.

23. Matsuda F.; Furusawa C.; Kondo T.; Ishii J.; Shimizu H.; Kondo A. Engineering strategy of yeast metabolism for higher alcohol production. *Microb Cell Fact* **2011**, 10(1):70. https://doi.org/10.1186/1475-2859-10-70.

24. Famili I.; Forster J.; Nielsen J.; Palsson B.O. *Saccharomyces cerevisiae* phenotypes can be

predicted by using constraint-based analysis of a genome-scale reconstructed metabolic network. *Proc Natl Acad Sci USA* **2003**, 100(23):13134–13139. https://www.ncbi.nlm.nih.gov/pubmed/14578455.

25. Orth J.D.; Thiele I.; Palsson B.Ø. What is flux balance analysis? *Nat Biotechnol* **2010**, 28(3):245-248. https://www.ncbi.nlm.nih.gov/pubmed/20212490.

26. Nissen T.L.; Schulze U.; Nielsen J.; Villadsen J. Flux Distributions in Anaerobic, Glucose-Limited Continuous Cultures of *Saccharomyces cerevisiae*. *Microbiology* **1997**, 143(1):203–18. http://mic.microbiologyresearch.org/content/journal/micro/10.1099/00221287-143-1-203.

27. Gonzalez R.; Andrews B.A.; Molitor J.; Asenjo J.A. Metabolic analysis of the synthesis of high levels of intracellular human SOD in *Saccharomyces cerevisiae* rhSOD 2060 411 SGA122. *Biotechnol Bioeng* **2003**, 82(2):152–69. https://doi.org/10.1002/bit.10556.

28. Sárvári Horváth I.; Franzén C.J.; Taherzadeh M.J.; Niklasson C.; Lidén G. Effects of furfural on the respiratory metabolism of *Saccharomyces cerevisiae* in glucose-limited chemostats. *Appl Environ Microbiol* **2003**, 69(7):4076–86. https://www.ncbi.nlm.nih.gov/pubmed/12839784.

29. Stephanopoulos G.N.; Aristidou A.A.; Nielsen J. *Metabolic Engineering: Principles and Methodologies,* San Diego: Academic Press., editor. 1998; pp. 154–196, ISBN:9780126662603.

30. SGD. *Saccharomyces cerevisiae* Genome Database. 2017. https://doi.org/www.yeastgenome.com.

31. Beltran G.; Novo M.; Rozès N.; Mas A.; Guillamón J.M. Nitrogen catabolite repression in *Saccharomyces cerevisiae* during wine fermentations. *FEMS Yeast Res* **2004**, 4(6):625–32. http://www.sciencedirect.com/science/article/pii/S1567135603002629.

32. Díaz-Montaño DM, Favela-Torres E, Córdova J. Improvement of growth, fermentative efficiency and ethanol tolerance of *Kloeckera africana* during the fermentation of Agave tequilana juice by addition of yeast extract. *J Sci Food Agric* **2009**, 90(2):321–8. https://doi.org/10.1002/jsfa.3820.

33. Gschaedler Mathis A.; Amaya Delgado L.; Arellano Plaza M.; Arrizon Gaviño J.; Herrera López E. J.; Iñiguez Muñoz L.; Kirchmayr M., La Fermentación: Etapa Clave en la Elaboración del Tequila. In *Ciencia y Tecnología del Tequila: Avances y Perspectivas*, 2nd ed.; CIATEJ, México, 2017; pp. 231–319, ISBN: 978-607-96619-8-4.